SURFACE PASSIVATION PROVIDED BY AN ALNEAL THROUGH SiO_2/TiO_2 BILAYER

K.A. Collett, M. Cyrson, R.S. Bonilla and P.R. Wilshaw
Department of Materials, University of Oxford
Department of Materials, University of Oxford, Parks Rd, Oxford, OX1 3PH

The process of annealing a SiO_2 dielectric layer coated in aluminium, termed the alneal, is known to produce some of the most effective surface passivation for silicon. However, it is traditionally performed on a SiO_2 dielectric coating which has sub-optimal anti-reflection properties. In this work it is shown that it is possible to achieve alneal passivation through a double layer SiO_2/TiO_2 stack. TiO_2 was investigated as it is one of the most effective anti-reflection coatings available and its deposition technology is advanced and cost effective. Here, the alneal was carried out on n-type ~40 Ωcm Cz-Si coated with a SiO_2/TiO_2 dielectric stack. In the best case, the alneal produced a lifetime increase from ~15 µs to 3084 µs, which equates to a SRV ≤ 10 cm/s or a J_{0e} of 32 fA/cm^2. This increase in lifetime was comparable to that achieved by a conventional alneal on a single layer SiO_2 specimen. It was also found that the thicker the TiO_2, the less effective the alneal was at passivating. Lastly, the passivation achieved after the alneal on the SiO_2/TiO_2 bilayer was found to be more stable than that achieved on the conventional single SiO_2 layer.
Keywords: surface passivation, silicon solar cell, dielectric coating.

1 INTRODUCTION

The silicon solar cell industry is beginning to adopt high efficiency back contact cell designs which are able to produce higher efficiencies [1], [2]. However, one major issue for back contact cells is that minority carriers generated near the silicon surface must diffuse a greater distance before reaching the p-n junction. Thus, the need for high quality surface passivation becomes far more significant. Recombination is prevalent at the silicon surface due to the abundance of bandgap states that exist as a result of lattice discontinuities. There are two aspects to passivation. Firstly, the number of inter-bandgap states can be reduced by chemically passivating the surface. Secondly, carrier access to the inter-bandgap states can be limited by means of an electric field, known as field effect passivation (FEP). Both of these passivation schemes can be provided by a dielectric capping layer. However, this is not the only job of this capping layer; it must also act as an anti-reflection coating (ARC) to improve the optical absorption efficiency of the cell. For this reason, the choice of capping layer, and the parameters used to deposit or grow it, must be optimised to achieve effective passivation and anti-reflection.

One of the most effective techniques to improve the passivation quality of the dielectric once it is in place is the so called *alneal* process. It was first developed by Eades [3] and later used by Kerr and Cuevas [4] to minimise surface recombination and characterise bulk recombination processes. The alneal is conventionally performed on SiO_2 [4] and, according to Kerr and Cuevas, is able to produce SRVs as low as 2.4 cm/s on 1.5 Ωcm n-type Si [4]. However, SiO_2 does not provide effective anti-reflection characteristics since the refractive index is too low [5] ($n = 1.46$ at $\lambda = 632$ nm [6]). If the high quality passivation provided by an alneal could be used on a superior ARC, the efficiency of the entire cell design would be improved. TiO_2 is a top quality anti-reflection coating for solar cells due to its high refractive index and low absorption [7]. Despite this, TiO_2 is no longer used in the silicon PV industry due to its poor passivation properties [5], [8]. One method to overcome this poor passivation is by using an intermediate SiO_2 layer that provides better chemical passivation. It is known that the passivation provided by a SiO_2 layer can be further improved by an alneal and thus the effectiveness of the alneal on a SiO_2/TiO_2 double layer dielectric is investigated in this work.

2 EXPERIMENTAL PROCEEDURE

Czochralski (Cz), ~ 40 Ωcm, n-type silicon wafers were dry oxidised at 900 ˚C to grow a 30 nm thermal SiO_2 layer. A SiO_2 layer of this thickness was required for certain characterisation techniques and further work will be done to investigate the impact of using a thinner SiO_2 layer. The wafer was then diced into 3 x 3 cm^2 samples, and batches of these were then deposited with TiO_2. Specimens with a single SiO_2 layer were kept in order to contrast the conventional alneal with that of the double layer. The TiO_2 was deposited in a thermal evaporator on both sides of the sample. The thickness of the resulting films was measured using a Vecco DekTak 6M stylus profiler.

The alneal was performed on both the single SiO_2 layer and double layer (SiO_2/TiO_2) specimens. In order to do this, the samples were coated, on both sides, with ~100 nm aluminium using a thermal evaporator. Controls without an aluminium coating accompanied both the SiO_2 and SiO_2/TiO_2 specimens for all processing except the thermal evaporation of the aluminium. All samples were annealed in a tube furnace in an argon atmosphere for 30 minutes at 400 ˚C. After annealing, the Al was etched off in HCl at 80 ˚C. The controls, without the Al coating, were also placed in the etchant. The process of etching the Al also removed the TiO_2 on the double layer specimens. This is believed to be due to the low temperature at which the TiO_2 was deposited, which resulted in poor adhesion of the TiO_2 film to the SiO_2 surface. Future work will investigate using APCVD deposited TiO_2. Sinton photo-conductance measurements were taken to calculate the lifetime of the specimens. All lifetime values are quoted at an injection level of 10^{15} cm^{-3}. The TiO_2 was deposited in several different batches in order to vary the thickness of the deposition. Each deposition batch was assigned a batch number and the characteristics of each are shown in Table I. The refractive index of one of the samples from batch 1 was measured using an optical reflectometer and it was found to be 1.96 at 632 nm.

Table I Batch characteristics of TiO_2 depositions

Batch Number	TiO_2 thickness (nm)	
	Front	Rear
1	66 ± 5.6	57 ± 2.5
2	133 ± 3.5	158 ± 22
3	89 ± 8.8	77 ± 19
4	109 ± 4.9	123 ± 5.7
5	82 ± 5	84 ± 10
6	105 ± 7	101 ± 9

3 PASSIVATION DUE TO TiO_2 DEPOSITION

After depositing the TiO_2 in the thermal evaporator the lifetime of each sample was recorded. These are shown in Table II along with the batch number for the TiO_2 deposition as described in Table I.

Table II: Lifetime of samples before and after TiO_2 deposition

SiO_2/TiO_2		SiO_2
Batch no.	Lifetime (µs)	Lifetime (µs)
1	15.72	12.56
1	16.04	12.80
2	18.00	14.49
2	17.83	12.94
3	15.13	12.91
4	13.23	12.27
4	16.34	13.02

The data in Table II shows that the addition of the TiO_2 layer on top of the SiO_2 causes a slight increase in lifetime. On average, the SiO_2/TiO_2 double layer samples have a lifetime ~3 µs greater than the SiO_2 single layer samples; this is an insignificant increase in lifetime.

4 ALNEAL ON SiO_2/TiO_2 stack

In order to alneal the samples, 100 nm of aluminium was thermally evaporated on top of the dielectric(s). As controls, both a single layer SiO_2 sample and a double layer SiO_2/TiO_2 sample were annealed without the aluminum layer.

Figure 1 shows the injection dependent minority carrier lifetimes for four samples after the anneal. The alnealed SiO_2/TiO_2 sample shown in Figure 1 was the one that demonstrated the best improvement from the alneal process. In this case the TiO_2 deposited was from batch 1. The other samples shown in Figure 1 were all annealed in the same process. The lifetimes achieved by other alnealed SiO_2/TiO_2 and SiO_2 samples are shown in Table III.

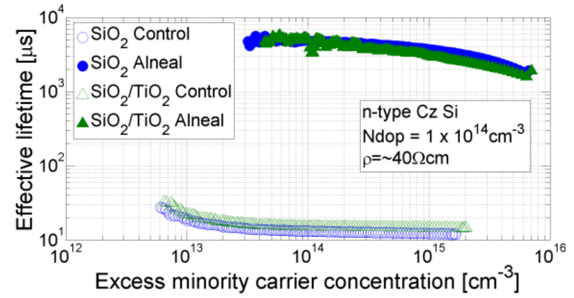

Figure 1 Effective lifetime vs minority carrier concentration curves for Cz ~40 Ωcm n-type Si with both alnealed (full symbols) and control (hollow symbols) SiO_2 (blue) and SiO_2/TiO_2 dielectrics (green). The TiO_2 on these samples was from batch 1 and ~ 62 nm thick.

From Table II and Figure 1 it is evident that both the controls, which were annealed in the tube furnace but were not coated in aluminium, achieved negligible change in lifetime. Both remained at their initial lifetimes of 12 µs and 15 µs for the SiO_2 single layer and SiO_2/TiO_2 double layer respectively. In contrast, the alnealed single layer SiO_2 sample reached a lifetime of 3691 µs, and the double layer SiO_2/TiO_2 specimen achieved a lifetime of 3084 µs.

Effective surface recombination velocity (SRV) was calculated as $SRV \leq (1/\tau_{eff} - 1/\tau_{bulk})W/2$ where W is the thickness of the silicon. It is assumed that the bulk lifetime is only limited by the Auger recombination (as calculated by Richter's parameterisation [9]) and the radiative recombination as modelled by Altermatt [10]. This leads to a SRV ≤ 8.9 cm/s and ≤ 10.7 cm/s at injection level 10^{15} cm^{-3} for the SiO_2 single layer and SiO_2/TiO_2 double layer alneal specimens respectively. This model assumes that recombination in the bulk due to defects is zero and therefore the calculated SRV must be considered to be an upper limit.

Emitter saturation current, J_{0e}, was calculated using Kane and Swanson's technique [9] for both alnealed samples. Effective lifetime was corrected using Richter's bulk lifetime model and values for J_{0e} were extracted directly from Sinton's lifetime software. Figure 2 shows the data used for this calculation. The saturation currents for the SiO_2 single layer and the SiO_2/TiO_2 double layer were calculated to be 32 fA/cm² and 33 fA/cm² respectively.

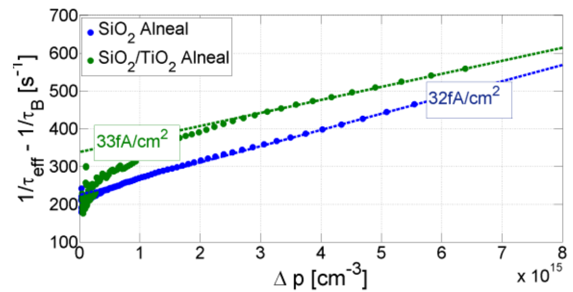

Figure 2 J_{0e} calculation using Kane and Swanson's method implemented in the Sinton lifetime software.

The alneal was repeated several times on both the single SiO_2 layer and the double SiO_2/TiO_2 layer samples. The lifetimes of these samples after alnealing are presented in Table III and the lifetime of the controls in Table IV.

Table III: Lifetime of samples after the alneal process at 400 ˚C for 30 minutes.

	SiO_2/TiO_2 Alneal		SiO_2 Alneal	
Batch no.	τ (μs)	SRV	τ (μs)	SRV
1	3084	10.7	3691	8.9
5	1506	22.2	4276	7.6
5	706	47.6	3593	9.1
6	312	108	3218	10.2

Table IV: Lifetime of samples after an anneal (with no aluminium) at 400 ˚C for 30 minutes.

	SiO_2/TiO_2 No Al		SiO_2 No Al	
Batch no.	τ (μs)	SRV	τ (μs)	SRV
1	15.5	2177	12.2	2766

5 EFFECT OF TiO_2 THICKNESS

It is clear from Table III that the minority carrier lifetime of the samples that underwent an alneal is significantly greater than the control samples that were simply annealed without any aluminium on the dielectric surface. Thus, one can conclude that the increase in lifetime is due to the presence of the aluminium during the anneal, and not the anneal itself.

When comparing the increase in lifetime between the double SiO_2/TiO_2 layer and the single SiO_2 layer, two points are evident. Firstly, the lifetimes achieved by the SiO_2/TiO_2 double layer samples are not as high as those achieved on the alnealed SiO_2 single layer samples. This could indicate that the TiO_2 presents a partial barrier to the mechanism by which the alneal process passivates the silicon surface. Secondly, the range in lifetimes achieved after the alneal is much greater for the SiO_2/TiO_2 double layer samples than for the single layer SiO_2 samples.

Previous reports by Zhao [11], Reed [12] and Cuevas [13] have suggested that the mechanism by which the alneal works is via hydrogen passivation. Hydrogen is said to be released due to aluminium interaction with hydroxyl ions present in the silicon dioxide [11]. This hydrogen is then free to diffuse and passivate dangling bonds at the silicon surface.

If this model is applied to the SiO_2/TiO_2 bilayer then there are two possible locations where the Al may react with hydroxyl ions, either within the SiO_2 or within the TiO_2. If the Al reacts with hydroxyl ions within the SiO_2, then the Al must diffuse through the TiO_2. If the reaction takes place within the TiO_2, any hydrogen produced in the TiO_2 would need to diffuse through both the TiO_2 and the SiO_2 (including the TiO_2/SiO_2 interface) in order to reach the silicon and passivate the surface. It is also possible that the TiO_2 layer may not be as rich in hydroxyl ions as the SiO_2 layer.

By varying the thickness of the TiO_2 layer, it is possible to assess whether the TiO_2 layer is acting as a diffusion barrier to the source of passivation or if a different mechanism limits the passivation. The average thickness of the TiO_2 layer against lifetime is shown in Figure 3.

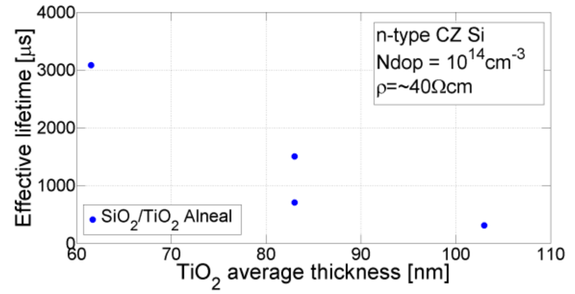

Figure 3 Effective lifetime at injection level of 1 x10^{15} cm^{-3} after alneal vs average TiO_2 thickness on SiO_2/TiO_2 double layer dielectric sample.

The results displayed in Figure 3 show that the thickness of the TiO_2 layer does have an effect on the effective lifetime after the alneal: the thicker the TiO_2 layer, the lower the effective lifetime. This supports the theory that the TiO_2 acts as a diffusion barrier to the source of passivation.

The variation between the two samples with a TiO_2 of 83 nm indicates that it is not only the TiO_2 thickness that affects the change in lifetime, there is another factor. This is corroborated by the variation seen in the results for the alnealed SiO_2 samples, where there is a difference of 1 ms for identically processed samples. One likely cause of this variation is a temperature profile within the tube furnace.

6 STABILITY OF LIFETIMES

The lifetimes of one of the alnealed single layer SiO_2 and double layer SiO_2/TiO_2 samples were monitored after the alneal. The TiO_2 deposition on the monitored sample was from batch 5 and ~ 83 nm. The stability of the effective lifetime curve with time is shown for each sample in Figure 4 (a) and (b).

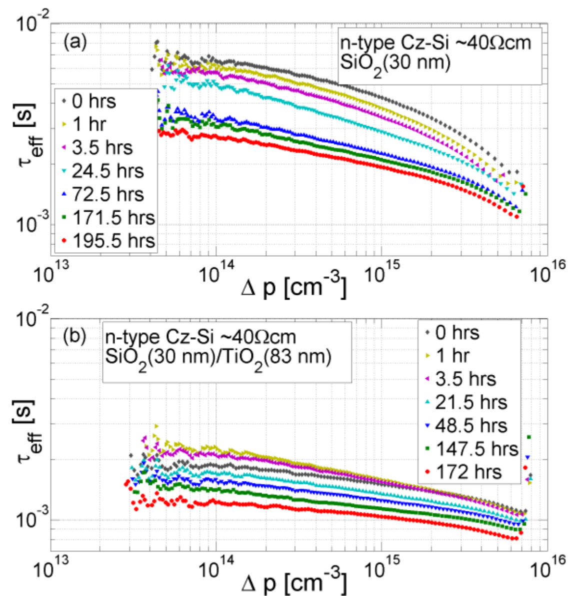

Figure 4 Effective lifetime vs minority carrier concentration at a given time after the alneal process on ~40 Ωcm Cz silicon with (a) a 30 nm SiO_2 dielectric and (b) a 30 nm SiO_2/ 83 nm TiO_2 dielectric stack

For clarity, the effective lifetime at a minority carrier concentration of 10^{15} cm^{-3} for both samples is shown against time in Figure 5. This data was used to extract the decay time constant and better define the lifetime stability.

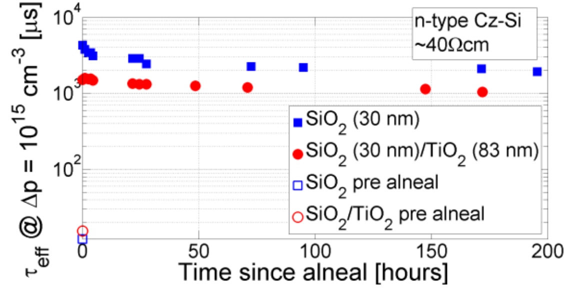

Figure 5 Effective lifetime at 10^{15} cm^{-3} against time after alneal of ~40 Ωcm Cz Si with a single SiO_2 layer (blue) and with a SiO_2/TiO_2 double layer dielectric (red).

From Figure 5 it is evident that the initial rate of decay in lifetime of the single SiO_2 dielectric layer is greater than of the SiO_2/TiO_2 bilayer. The decay time constants for the two curves (after the initial rapid decay) were calculated and found to be 20.4 days and 38.2 days for the SiO_2 and SiO_2/TiO_2 double layers respectively.

7 IMPACT OF ETCHING

It was observed that the decay in lifetime began only after the aluminium and TiO_2 had been removed in HCl at 80 ˚C and the samples rinsed in DI water. This was found by alnealing two samples, from the same TiO_2 deposition batch, together. One of these samples was etched immediately after the alneal. The other was stored, with the aluminium and TiO_2 intact, for a week before it was also etched. The lifetimes of both samples were monitored from immediately after etching. The results of this are shown in Figure 6. The samples used were from batch 6 with an average of 103 nm of TiO_2.

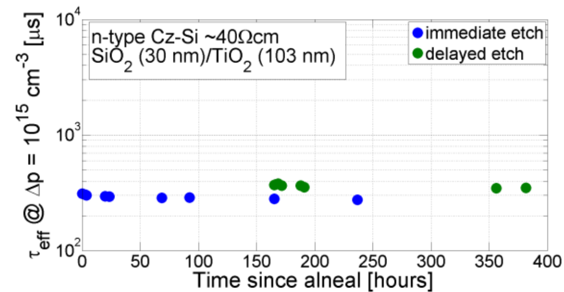

Figure 6 Lifetime vs time after alneal for a sample where the Al and TiO_2 were etched immediately after the alneal (blue) and another sample where the Al and TiO_2 were not etched until a week after the alneal (green).

A pair of single layer SiO_2 samples underwent the same procedure. The results of this are shown in Figure 7.

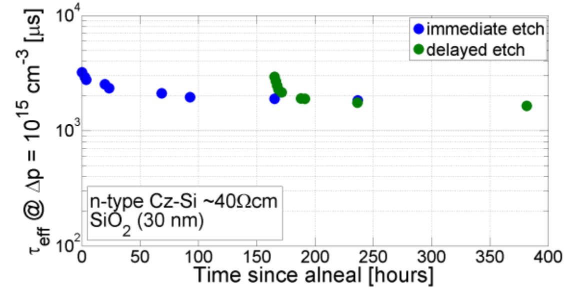

Figure 7 Lifetime vs time after alneal for a sample where the Al was etched immediately after the alneal (blue) and another sample where the Al was not etched until a week after the alneal (green).

From Figure 6 and Figure 7 it is evident that the lifetime decay is stimulated when the aluminium covering the samples is etched and the samples rinsed in DI water. The difference in the starting lifetime values for the samples in both Figure 6 and Figure 7 are most likely due to temperature variation within the furnace.

The possibility that the lifetime decay is caused by light irradiation was investigated. Twin samples, with a single layer SiO_2 dielectric, were processed identically. They were both etched immediately after the alneal. After etching, one was kept in the dark between lifetime measurements; the other was kept on the benchtop in a transparent plastic bag. The lifetimes of both were monitored with time and are shown in Figure 8.

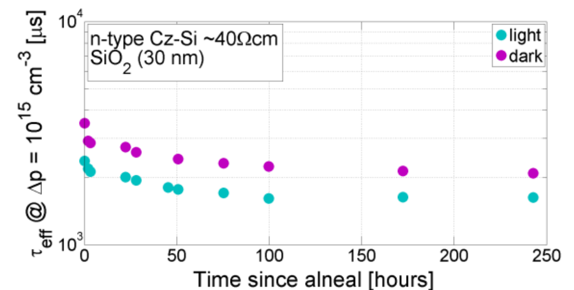

Figure 8 Lifetimes with time since alneal for SiO_2 coated ~40 Ωcm Cz silicon samples kept in the dark (purple) and kept in a transparent bag on the benchtop (teal)

As the decay rates of the two curves are very similar, it can be concluded that light is not the cause of the lifetime decay.

The trigger for the decay is not yet understood, however, two possibilities are that either the decay is stimulated by the wet processing itself or that the wet processing introduces a further source of passivation that decays with a shorter time constant.

8 CONCLUSIONS

It has been demonstrated that the effective passivation process of annealing SiO_2 passivation layers coated with aluminium, known as the alneal, is also possible on SiO_2/TiO_2 double layers. In this work the most effective alneal was seen to improve the lifetime of the n-type ~40 Ωcm Cz-Si coated in a SiO_2/TiO_2 double layer dielectric from ~15 µs to 3084 µs at 10^{15} cm^{-3}. This equates to a SRV ≤ 10 cm/s or a J_{0e} of 32 fA/cm^2. The thickness of the TiO_2 dielectric layer was seen to affect the post-alneal lifetime of the sample indicating that the

TiO_2 is likely acting as a diffusion barrier to the source of passivation. The stability of the passivation was also monitored. It was seen that the alneal passivation on the SiO_2 dielectric decayed at a greater rate than the passivation on the SiO_2/TiO_2 dielectric layer. The decay rates were calculated to be 20.4 days and 38.2 days on the single and double layer samples respectively. The major advantage of this finding to the solar cell industry is that this provides a method by which the excellent anti-reflection properties achieved by TiO_2 coatings could once again be exploited.

ACKNOWLEDGMENTS

K A Collett would like to thank EPSRC for funding her doctoral studies. Thanks also go to the Armourers and Brasiers Gauntlet Trust and Supergen Super Solar for travel grants to attend EUPVSEC. R S Bonilla is the recipient of an EPSRC (UK) Postdoctoral Research Fellowship, EP/M022196/1. P R Wilshaw acknowledges the support from EPSRC grant EP/M024911/1. Data published in this article can be downloaded from http://ora.ox.ac.uk. All authors are thankful to Martin Hermle and Christian Reichel at Fraunhofer ISE for provision of silicon material, and to Radka Chakalova for her extensive help in the cleanroom.

REFERENCES

[1] S. Pukhrem, “Concepts In Photovoltaic Technology,” *Solar Love*, 2014. [Online]. Available: http://solarlove.org/concepts-photovoltaic-technology/. [Accessed: 08-Apr-2015].

[2] “SunPower Sets Solar Cell Efficiency Record at 24.2% - Renewable Energy World.” [Online]. Available: http://www.renewableenergyworld.com/articles/2010/06/sunpower-sets-solar-cell-efficiency-record-at-24-2.html. [Accessed: 10-Sep-2015].

[3] W. D. Eades, “PhD Thesis,” Stanford University, 1985.

[4] M. J. Kerr and A. Cuevas, “Very low bulk and surface recombination in oxidized silicon wafers,” vol. 35, pp. 13–17, 2002.

[5] B. S. Richards, “Comparison of TiO2 and other dielectric coatings for buried-contact solar cells: A review,” *Prog. Photovoltaics Res. Appl.*, vol. 12, no. 4, pp. 253–281, 2004.

[6] “Refractive Index of SiO2, Fused Silica, Silica, Silicon Dioxide, Thermal Oxide, ThermalOxide for Thin Film Thickness Measurement.” [Online]. Available: http://www.filmetrics.com/refractive-index-database/SiO2/Fused-Silica-Silicon-Dioxide-Thermal-Oxide-ThermalOxide. [Accessed: 04-Feb-2016].

[7] K. Ali, S. A. Khan, and M. Z. M. Jafri, “Effect of Double Layer (SiO 2 / TiO 2) Anti-reflective Coating on Silicon Solar Cells,” vol. 9, pp. 7865–7874, 2014.

[8] B. S. Richards, J. E. Cotter, and C. B. Honsberg, “Enhancing the surface passivation of TiO2 coated silicon wafers,” *Appl. Phys. Lett.*, vol. 80, no. 7, pp. 1123–1125, 2002.

[9] A. Richter, S. W. Glunz, F. Werner, J. Schmidt, and A. Cuevas, “Improved quantitative description of Auger recombination in crystalline silicon,” *Phys. Rev. B - Condens. Matter Mater. Phys.*, vol. 86, no. 16, pp. 1–14, 2012.

[10] P. P. Altermatt, F. Geelhaar, T. Trupke, X. Dai, a. Neisser, and E. Daub, “Injection dependence of spontaneous radiative recombination in crystalline silicon: Experimental verification and theoretical analysis,” *Appl. Phys. Lett.*, vol. 88, no. 26, 2006.

[11] J. Zhao, A. Wang, P. P. Altermatt, S. R. Wenham, and M. A. Green, “24% Efficient Silicon Solar Cells,” pp. 1477–1480, 1994.

[12] M. L. Reed and J. D. Plummer, “Chemistry of Si-SiO2 interface trap annealing,” *J. Appl. Phys.*, vol. 63, no. 12, pp. 5776–5793, 1988.

[13] A. Cuevas, P. A. Basore, G. Giroult-Matlakowski, and C. Dubois, “Surface recombination velocity of highly doped n-type silicon,” *J. Appl. Phys.*, vol. 80, no. 6, pp. 3370–3375, 1996.